

Deformation Mechanism of Strained Polydiacetylene Single Crystal Viewed from the Molecular Level

Kohji Tashiro

*Department of Macromolecular Science, Graduate School of Science,
Osaka University, Toyonaka, Osaka 560, Japan*

ABSTRACT: Deformation mechanism of polydiacetylene single crystal [poly(1,6-di(*N*-carbazolyl)-2,4-hexadiyne, PDCHD)] under the application of tensile force along the chain axis has been investigated by means of the combination of lattice dynamical theory with the infrared/Raman spectroscopic and X-ray structural analytical techniques. The lattice dynamical theory predicted that, when the planar-zigzag chain of PDCHD is stretched along the chain axis, the skeletal chain should be deformed mainly through the stretching of the bond lengths and the opening of the bond angles but without any contribution of the torsional angle deformation. This theoretical prediction was first experimentally proven by the measurement of the stress-induced shifts of the vibrational frequencies of the infrared and Raman bands. These shifts were interpreted reasonably in terms of the anharmonicity of the force constants. The strain-induced atomic displacements were obtained more directly through the refined X-ray structural analysis made for the polydiacetylene single crystal subjected to the tensile stress.

Introduction

It is quite important to clarify the relationship between the structure and the mechanical properties of polymer materials because such an information is useful for the development of new polymer materials with more excellent mechanical properties. In particular the structure-property relationship of the crystalline region is important because the crystalline region may be assumed to be the ultimate state of the polymer substances.

For these twenty years, we have investigated the structure-mechanical property relationship for the polymer crystals, especially by focusing on the three-dimensional elastic constants.^{1,2} Even now, however, there are several problems still yet to be solved in these researches. For example, when we try to measure the crystallite modulus along the chain axis by the X-ray diffraction method under tension, we have to assume that the stress working on the crystalline region is equal to the externally-applied bulk stress, i.e., the mechanical series model of the amorphous and crystalline phases in the bulk sample. This assumption cannot be applied to any types of polymer samples.³⁻¹¹ It is

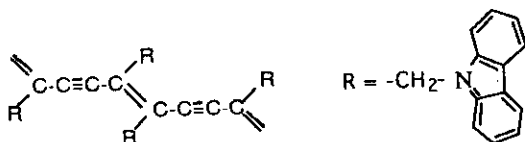
better to use the polymer materials where it is as highly crystalline and highly oriented as possible. The ultradrawn polyethylene and polyoxymethylene samples may satisfy this requirement. Unfortunately, however, strictly speaking, even for these samples, this assumption cannot be perfectly realized instead some heterogeneous distribution of stress is needed for the interpretation of the crystallite modulus¹¹.

For a more ideal case, therefore, we need to use "perfect single crystals" of polymers with a size large enough for manual treatment. This requirement cannot be satisfied practically for the general semicrystalline polymers. But we have one exceptional polymer, polydiacetylene, which can be obtained by the solid state polymerization of the monomer single crystal by irradiating γ -ray at room temperature.¹² The length of the obtained single crystal is several cm long, along the chain axis and can be treated by hand. In this paper we will describe the changes of the infrared/Raman spectra and X-ray diffraction pattern induced by tensile stress which was applied to the polydiacetylene "giant" single crystal, in order to clarify the structural change of this polymer chain that

was viewed from the molecular level.

Experimental

Sample. Monomer used here was the diacetylene with the *N*-carbazolyl groups as side chains. The needle-like single crystals were grown slowly from a toluene solution at room temperature, which were polymerized in the solid state by an irradiation of ^{60}Co γ -ray (40 Mrad) at room temperature. Thus the obtained polymer [poly(1,6-di(*N*-carbazolyl)-2,4-hexadiyne, PDCHD) single crystal has needle-like shape with a dimension of 30 mm length and 0.1 mm width, as shown in Figure 1. The uniform single crystals were picked out under an optical microscope and supplied to the experiments. The cross-sectional area of the crystal was homogeneous, allowing us to apply a uniform stress (or strain) over the whole sample.



Stress-Strain Curve. The crystallite modulus of semi-crystalline polymers is generally evaluated by the X-ray diffraction measurement under tension. But, in the case of PDCHD single crystal, a more convenient method is by measuring the stress-strain curve of the bulk sample; as shown in Figure 2 (a), the sample was hung vertically with a weight applied and the extension of the sample length was measured by a direct observation under an optical microscope. The temperature could be

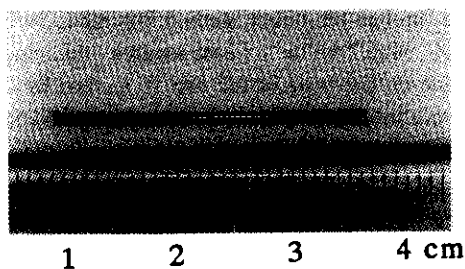


Figure 1. A photograph of PDCHD giant single crystal. The scale between a couple of major ticks is 1 cm.

changed arbitrarily by using the heater surrounding the sample.¹³

FTIR/Raman Spectral Measurements under Tension. For the measurements of the vibrational spectra of PDCHD under tension, the home-made cell shown in Figure 2 (b) was used.¹³ The sample was set horizontally. One end of the sample was fixed at the holder and the other end was drawn by applying a weight through a set of pulleys, which could enlarge a small weight to the larger force by a principle of lever. The polarized Fourier-transform infrared (FTIR) spectra were measured in a transmission fashion [Japan Spectroscopic Co. Ltd., FTIR-5MP]. The Raman spectra were measured by irradiating a He-Ne laser beam as an excitation light source and the 90° scattered signals were collected by a photomultiplier [Japan Spectroscopic Co. Ltd., R800].

X-ray Diffraction Measurement under Tension. The single crystal was set to the home-made sample stretcher as shown in Figure 2(c).¹⁴ Both ends of the sample were fixed at the holder and the sample was strained by carefully rotating the screw. The sample was placed under tension at a constant strain, during which the X-ray measurement was made. This *constant strain* mode is different from the above-mentioned *constant stress* mode used in the measurements of the IR and Raman spectra. In the case of general synthetic polymers, some stress relaxation occurs frequently when the samples are subjected to the *constant strain*, which makes the strain behaviour ambiguous because of stress relaxation during the experiment. In the case of the PDCHD single crystal, however, such a stress relaxation may not be considered to occur, because the stress-strain relation obeys almost perfectly to the so-called Hookian law, as shown later; in other words, this polymer crystal is considered to exhibit an almost perfect energy elasticity.

The X-ray diffraction data were collected by using an imaging plate (IP) system DIP3000 developed by MAC Science, Ltd., Japan. The IP system was chosen for the present experiment because the IP gives two-dimensional X-ray diffraction pattern and so we only need to oscillate the sample around one axis (ω axis), enabling us to mount the sample stretcher (see Figure 2 (c)).

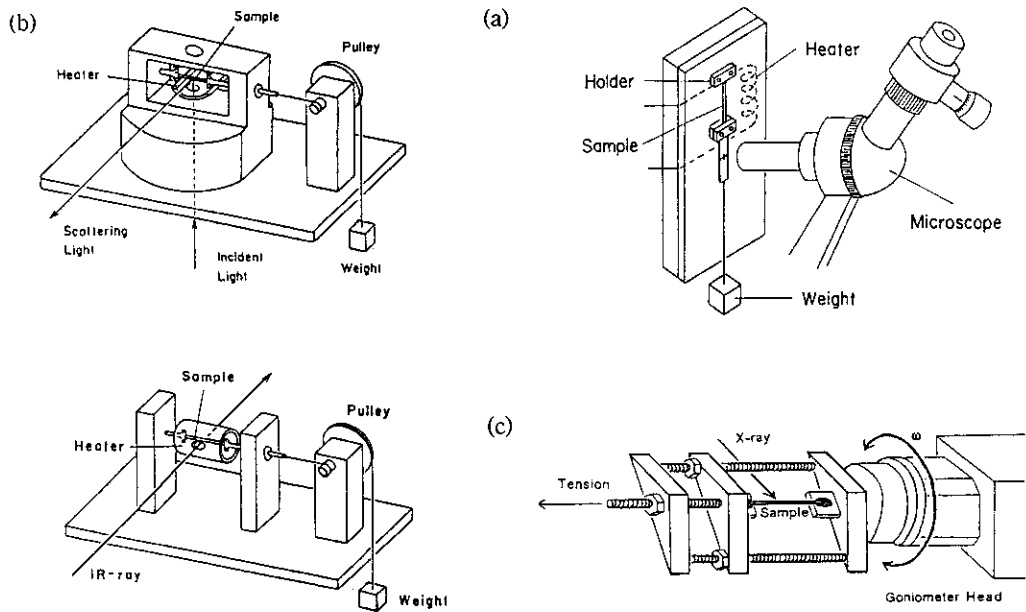


Figure 2. An illustration of sample stretchers for the measurements of (a) stress-strain curve, (b) infrared and Raman spectra, and (c) X-ray oscillation photographs.

This design is quite different from the auto 4-circle diffractometer in which the sample has to be rotated in a complex manner, around the ϕ and χ axes (the ϕ axis is a spindle axis of the sample and the χ axis is a tilt angle along the meridional line), making it difficult to hold the relatively heavy and bulky sample stretcher. A total of 20 shots of quasi-Weissenberg photographs with an oscillation angle ($\Delta\omega$) of 5° and a translation width of 1 cm were taken in the range of $\omega = 0\sim 100^\circ$ at a constant strain, where a graphite-monochromatized Mo-K α radiation ($\lambda = 0.71073 \text{ \AA}$) was used as an incident X-ray source (50 kV, 200 mA). The 5~7 sets of 20 Weissenberg photographs were taken for the sample with the same strain in order to evaluate the accuracy of the analyzed results and the experimental errors. The exposure time of one shot was 10 min and only about 3.5 hrs were needed to collect a set of photographs.

Structural Analysis. For the indexing of reflections and the integration of the intensity, computer softwares "DENZO" and "XDISPLAYF" were used.^{15,16} DENZO can index the diffraction pattern, and refine the crystal lattice parameters and detector parameters such as the rotation axis of the

sample, the center position of the oscillation, etc. and integrate the diffraction intensity. XDISPLAYF can compare the observed IP pattern with the reflection spots calculated by using the fitted parameters which are obtained and refined in the course of data analysis by DENZO. The total number of the observed reflections was about 6000, from which the effective and independent reflections, about 2300, were extracted ($0 < h < 18$, $0 < k < 4$, and $-24 < l < 23$). On the basis of the collected reflectional data, another software, "SCALEPACK", was used to determine more accurate lattice parameters and the scale factors between the successive frames of photograph, from which the accurately corrected data of structure factor were obtained. The structural analysis through the direct method was made on the basis of MULTAN78.¹⁷ Least-squares refinement was made on the basis of full matrix method by using the quantity $\sum w(|F_o|^2 - |F_c|^2)^2$ as a minimized function with the weight $w = \exp[FA \sin^2 q / (\lambda^2 \sigma^2(F_o))]$ where the $\sigma^2(F_o)$ is the squared standard error of the observed structure factor and the coefficient FA was set to the value 0.001. The reflections used in the least-squares calculation were about 1300 with the data reduction cut-off of $|F_o| \geq 3\sigma(|F_o|)$. Final

reliability factors were $R = 0.04-0.05$ and $R_w = 0.04-0.05$ for all the samples, where the R and R_w are defined as follows: $R = \Sigma||F_o| - |F_c||/\Sigma|F_o|$ and $R_w = \sqrt{\Sigma_w(|F_o| - |F_c|)^2/\Sigma_w|F_o|^2}$.

Result and Discussion

Lattice-Dynamical Prediction of Deformation Mechanism. The Young's modulus of polymer crystal along the chain axis is almost decided by the intramolecular interactions and the contribution of the intermolecular interactions is appreciably small. Therefore, under a good approximation we may calculate the Young's modulus along the chain axis by taking into account only the intramolecular interactions, that is, for the isolated single chain.¹ As one of the calculation methods of the elastic constants, the lattice dynamical theory is useful to understand the macroscopic physical property from the microscopic point of view on a basis of concrete crystal structure and interatomic interactions. The Young's modulus along the chain axis is expressed as follows.

$$E_c = [F_\epsilon - \tilde{F}_{\rho\epsilon}(F_\rho)^{-1}F_\rho\epsilon]/\nu \quad (1)$$

$$\begin{aligned} \text{where } F_\rho &= \tilde{B}_\rho F_R B_\rho \\ F_{\rho\epsilon} &= \tilde{B}_\rho F_R B_\epsilon \\ F_\epsilon &= \tilde{B}_\epsilon F_R B_\epsilon \\ B_\epsilon &= B_\rho W \end{aligned}$$

F_R is the force constant matrix representing the interatomic interactions. B_ρ is the transformation matrix between the internal displacement vector ΔR [including the bond stretching Δr , bond angle deformation $\Delta\phi$, internal torsional angle change $\Delta\tau$ and so on] and the Cartesian displacement vector ΔX : $\Delta R = B_\rho \Delta X$. W is the matrix consisting of the Cartesian coordinates of the constituent atoms. ν is the effective volume of a basic monomeric (or crystallographically asymmetric) unit. The B , B_ρ and B_ϵ matrices are calculated on the basis of the atomic coordinates and the F_R , F_ρ , $F_{\rho\epsilon}$, and F_ϵ matrices are calculated by employing suitable force field such as valence force field, Urey-Bradley force field, and so on.

The lattice dynamics can predict not only the crystallite modulus E_c but also the atomic dis-

placements induced by the application of the external force. The atomic displacement coordinate ΔX is calculated by the equation

$$\Delta X = W_\epsilon + \rho = [W - (F_\rho)^{-1}F_{\rho\epsilon}]\epsilon \quad (2)$$

where each atom is originally assumed to be displaced along the chain axis by an amount proportional to the product of W and strain ϵ (affine deformation, the first term of Eq 2) but such an "external deformation" is not necessarily the most advantageous, energetically, and the atoms change their relative positions to minimize as effectively as possible the externally applied deformation. This additional displacement of the atoms is called the internal strain ρ , which can be obtained under the condition of energy minimum at ρ (the second term in Eq 2). Similarly, the internal displacement coordinate vector ΔR is given by

$$\Delta R = B_\rho \Delta X = [B_\epsilon - B_\rho(F_\rho)^{-1}F_{\rho\epsilon}]\epsilon \quad (3)$$

This lattice-dynamics method also can calculate the vibrational frequencies of the crystal: the dynamical equation for the normal modes is expressed as

$$D_x L_x = L_x \Lambda_x$$

where Λ_x is an eigenvalue matrix, L_x is an eigenvector, and the dynamical matrix D_x is expressed as

$$D_x = \tilde{M}^{-1/2} \tilde{B}_\rho F_R B_\rho M^{-1/2} \quad (4)$$

In this equation, M is a diagonal matrix consisting of atomic masses. The wavenumber ν is given as follows by using the eigenvalue λ .

$$\nu = 1302.9\sqrt{\lambda} \text{ (cm}^{-1}\text{)} \quad (5)$$

Therefore, by comparing the calculated vibrational frequencies with the observed values, we can check whether or not the used force field is suitable (and the molecular geometry). The spectroscopically guaranteed force field and structure can lead to more reliable calculated results of the Young's modulus.

The above-mentioned lattice dynamical calculation was performed for PDCHD chain.¹³ The force constants were determined so that the calculated vibrational frequencies are in agreement

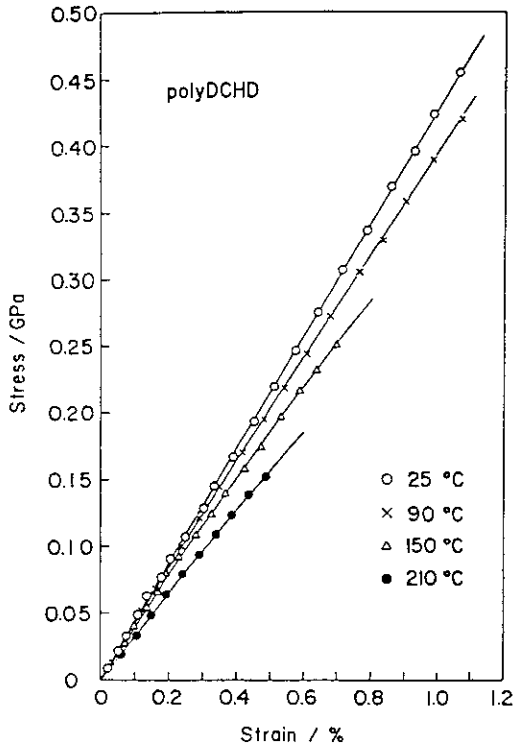


Figure 3. Stress-strain curves of PDCHD giant single crystal measured at the various temperatures.¹³

with the observed ones. The calculated modulus E_c for PDCHD is 41.1 GPa. Figure 3 shows the stress-strain curve measured for PDCHD, from the slope of which the observed Young's modulus is evaluated to be 43.2 GPa at room temperature. The calculated value is in good agreement with the observed value.

Figure 4 shows the atomic displacements and the distribution of the strain energy (SED) to the various internal coordinates, which were also calculated on the basis of Eq 3. The SED is defined as follows and indicates how largely the internal displacement coordinates contribute to the deformation of the chain.

$$\text{SED}(\%) \text{ for the } i\text{-th coordinate} = 100 \times F_i \Delta R_i^2 / \sum F_i \Delta R_i^2 \quad (6)$$

In the case of PDCHD, the bond stretching and bond angle deformation of the skeletal chain contribute mainly to the stretching of the planar-zigzag chain under the application of the tensile force.

Spectroscopic Proof of the Theoretically-Pre-

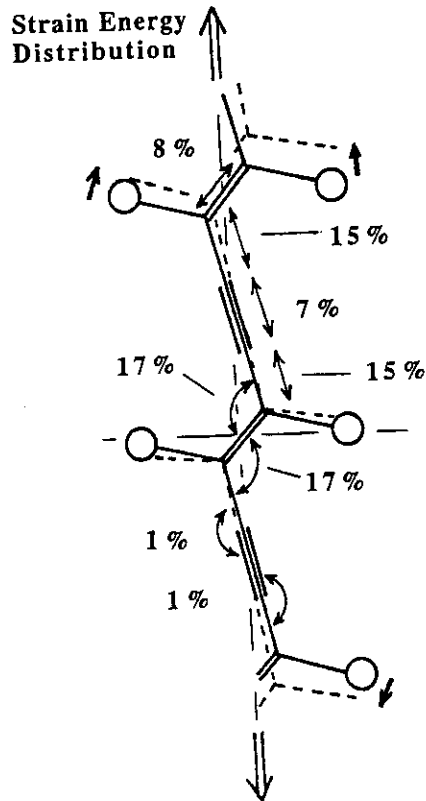


Figure 4. Atomic displacements and potential energy distributions calculated for polydiacetylene chain subjected to a hypothetically large tensile strain of 10%.¹³

dicted Chain Deformation Mechanism. The lattice dynamics predicted the atomic displacement of the PDCHD chain which was subjected to the tensile force as shown in Figure 4. This theoretical prediction needs to be confirmed through the experimental evidence. For example, vibrational spectra are very sensitive to slight changes in local structure. That is to say, the changes in bond lengths, bond angles, internal rotation angles and so on, and the changes in the corresponding force constants can be traced accurately by measuring the changes in frequency, intensity and breadth of vibrational bands. Therefore, vibrational spectroscopy is expected to be one of the most powerful methods to evaluate the stress-induced slight changes in structure and interactions and to deduce molecular deformation mechanisms of polymer crystals.^{1,18-20}

Figure 5 shows the Raman spectral change

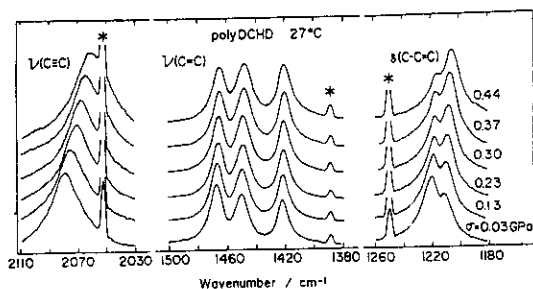


Figure 5. Raman spectral change of PDCHD crystal measured under tensile stress.¹³ Asterisks are emissions from Neon lamp to check the wavenumber drift.

measured for PDCHD under an application of tensile load.^{13,21,22} This polymer has an absorption peak of visible-ultraviolet spectra around 660 nm, and the obtained spectra are so-called resonance Raman spectra, where only the vibrational modes associated with the skeletal electronic conjugation system (stretching modes of double and triple bonds, etc.) were detected when the incident laser with 632.8 nm wavelength was used as an excitation light source. The peak position of the bands was found to shift clearly to the lower frequency side with increasing tensile stress. The profile change was also observed in the frequency regions of 1500–1400 and 1260–1200 cm^{-1} , which comes from the change in the vibrational coupling between the skeletal and side-group modes. The skeletal modes with high frequency shift factors $[\partial\nu/\partial\sigma]$ corresponded well to those of high SEDs, predicted for the stressed PDCHD chain (Figure 4): the C=C stretching $[\nu(\text{C}=\text{C})]$, C \equiv C stretching $[\nu(\text{C}\equiv\text{C})]$ and C-C=C bending $[\delta(\text{CCC})]$ modes. The calculation predicts a high SED to the skeletal C-C single bond, therefore we may expect a large frequency shift for the corresponding C-C stretching band $[\nu(\text{CC})]$. This $\nu(\text{CC})$ is Raman inactive, as known from the factor group analysis and we need to search the band in the infrared spectra. Although the measurement was difficult for a thin and small single crystal of PDCHD, as long as the conventional dispersion-type infrared spectrometer was used, the FTIR spectroscopy lead to a success in the measurement of the polarized infrared transmission spectra of PDCHD single crystal.¹³ Figure 6 shows the obtained FTIR spectral change, induced by the tensile stress. Both the vibrational

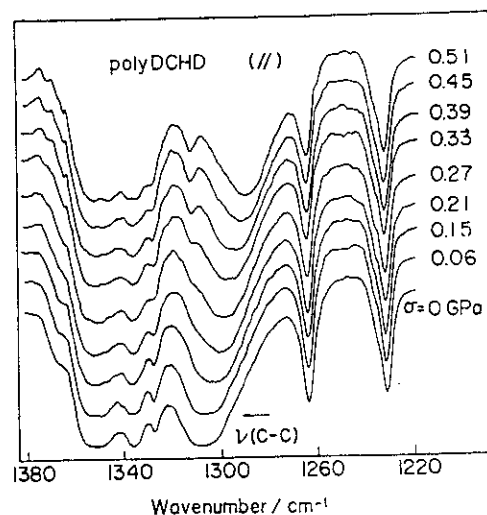


Figure 6. FTIR change of polydiacetylene thin crystal measured under tensile stress (the parallel component).¹³

bands of the main chain and side groups were infrared active and so the spectra were very complicated. Among these many infrared bands, only one band locating at ca. 1307 cm^{-1} was found to show a large frequency shift ($-31 \text{ cm}^{-1}/\text{GPa}$). The normal modes calculation revealed this band assignable to the antisymmetric skeletal C-C stretching mode $\nu_{as}(\text{C}-\text{C})$. Figure 7 summarizes the stress dependence of the vibrational frequencies of the detected Raman and infrared-active skeletal modes.

At this stage we have a question: Why does such a vibrational frequency shift occur for the deformation of the chains? A vibrational frequency shift has been explained in terms of the anharmonicity of the vibration.²³⁻²⁶ The lattice dynamical method was adopted to the problem of stress-induced vibrational frequency shift of polymer crystals under the quasiharmonic approximation. As shown in eqs 4 and 5, the vibrational frequency ν can be obtained by solving the dynamical equation which is a function of force constants, molecular (and crystal) structure and atomic masses. The external stress may cause the structural deformation, which affects the intramolecular (and intermolecular) force fields and then the frequency ν . We assume here that the internal coordinates (bond length, bond angle, etc.) will change from R_i to R as a result of deformation of the crystal. The mechanical strain energy V of

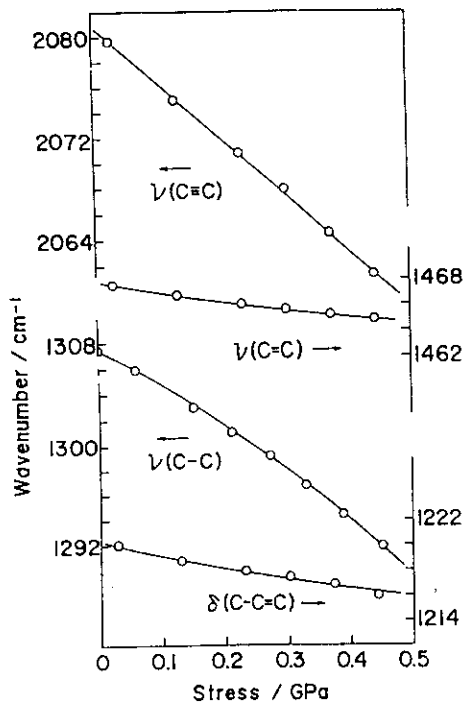


Figure 7. Stress dependence of the vibrational frequencies measured for PDCHD sample crystal.¹³

the system is expressed by

$$V = V_0 + \Sigma(\partial V / \partial R_i)_0 \Delta R_i + (1/2) \Sigma \Sigma (\partial^2 V / \partial R_i \partial R_j)_0 \Delta R_i \Delta R_j + (1/3!) \Sigma \Sigma \Sigma (\partial^3 V / \partial R_i \partial R_j \partial R_k)_0 \Delta R_i \Delta R_j \Delta R_k + \dots \quad (7)$$

Here ΔR is that defined in Eq 3 and should be distinguished from ΔR_{ib} , the internal displacement coordinate for representing the vibrationally caused displacement of bond length, bond angle, etc. Assuming V_0 equal to zero and employing the condition $(\partial V / \partial R)_0 = 0$, the above equation can be rewritten as follows.

$$V = (1/2) \Sigma \Sigma [(\partial^2 V / \partial R_i \partial R_j)_0 + (1/3) \Sigma (\partial^3 V / \partial R_i \partial R_j \partial R_k)_0 \Delta R_k] \Delta R_i \Delta R_j + \dots \approx (1/2) \Sigma \Sigma F_{ij} \Delta R_i \Delta R_j \quad (8)$$

where

$$F_{ij} = (\partial^2 V / \partial R_i \partial R_j)_0 + (1/3) \Sigma (\partial^3 V / \partial R_i \partial R_j \partial R_k)_0 \Delta R_k = F_{ij}^0 + \Sigma F'_{ijk} \Delta R_k \quad (9)$$

Equation 8 corresponds formally to the expression

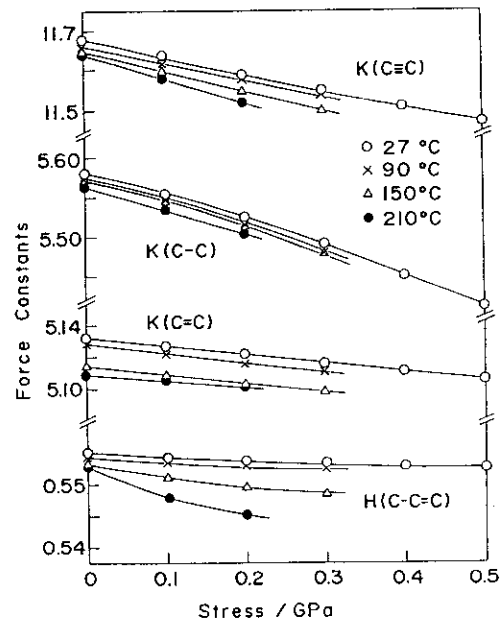


Figure 8. Stress dependence of the force constants estimated for PDCHD sample.¹³

of the harmonic potential energy with the force constant F_{ij} but the F_{ij} is affected by the change in the internal coordinates ΔR_k . This kind of treatment is reasonable for an infinitesimally small change of R and called a "quasiharmonic approximation". Since the internal displacement coordinates ΔR_k are expressed as a linear function of the stress σ or strain ϵ (Eq 3), we have the following expression for F_{ij} :

$$F_{ij} = F_{ij}^0 + F'_{ij} \sigma \quad (10)$$

That is, the force constants are expressed as a function of σ .

In the actual analysis of the spectroscopic data, the diagonal components of the force constants were determined by the least squares method so that the calculated vibrational frequencies would be as close to the observed values as possible. The obtained stress-dependence of the diagonal force constants is plotted in Figure 8, where an effect of temperature is also included.

As seen from the comparison of Figure 4 with Figure 7, the vibrational modes with large frequency shift correspond to the internal displacement coordinates to which the strain energy is largely distributed. What type of quantitative re-

relationship is existent between the SED and the frequency shift $\Delta\nu$? The development of the equations derived under a quasi-harmonic approximation gives the following expression for the frequency shift $\Delta\nu$:

$$\Delta\nu \propto B_p F' \sqrt{SED} / F_0 \quad (11)$$

where B_p , F_0 and F' are the components of the B and F matrices (F_0 : harmonic component and F' : anharmonic component). $\Delta\nu$ is proportional to \sqrt{SED} and so we can interpret why only the vibrational frequencies of the skeletal modes are shifted appreciably by the application of tensile stress. Equation 11 can be rewritten as

$$\Delta\nu \propto B_p (\partial d / \partial R) F' / \sqrt{F_0^3} \quad (12)$$

where $(\partial d / \partial R)$ is the elongation of the helical pitch d (or the repeat period along the chain axis) per unit change in the internal coordinate R . The wavenumber shift $\Delta\nu$ is governed by the product of the geometrical factor $B(\partial d / \partial R)$ and the interaction factor $F' / (F_0)^{3/2}$. In other words, the vibrational mode with soft (small) force constants F_0 and high anharmonicity F' shifts largely but the degree is also determined by the geometrical factor (or the conformation of the polymer chain).

Refined X-ray Structural Analysis of the Deformed PDCHD Chain. In this way, the infrared and Raman spectroscopic methods could supply very important informations on the atomic displacements in a form of vibrational frequency shifts. Based on the lattice dynamical theory developed under a quasiharmonic approximation, we were able to clarify the quantitative relationship between the frequency shifts and the atomic displacements (Eqs 11 and 12) by assuming that the force constants were modified through the changes in the internal coordinates such as the bond lengths, bond angles and/or internal torsional angles (Eqs 9 and 10).

At this stage, however, we have to realize that the vibrational spectroscopic interpretation of the mechanically deformed polymer crystals has a limitation to getting a direct information concerning the atomic displacements. This is because the vibrational frequency is a function of the force constants and the atomic coordinates in a complicated

manner. In order to obtain more direct and definite information concerning the atomic displacements, we have to necessarily rely on the refined crystal structural analysis by using the X-ray diffraction technique. In general, the polymer crystals show quite a poor X-ray diffraction pattern, consisting of a small number of broad reflections, making it difficult to utilize the "direct" method employed frequently in the refined structural analysis of low-molecular-weight compounds. This situation makes it practically impossible to detect the quite small atomic displacements occurring in the deformed polymer crystal. We need to obtain a single crystal of polymer which is large enough to be treatable manually. Then, we can utilize the PDCHD single crystal as a candidate for the above-mentioned purpose, i.e., a direct experimental proof of molecular deformation mechanism. Concretely speaking, this PDCHD sample was tensioned uniaxially by using the home-made stretcher, which was mounted on the goniometer head and the sets of X-ray oscillation photographs were taken by using the imaging-plate (IP) system. The refined structural analysis was made for the collected IP data and the change in the unit cell parameters, as well as, the atomic positions were evaluated.¹⁴

Strain-induced Change of Unit Cell Parameters of PDCHD. In Figure 9 the molecular and crystal structures of PDCHD analyzed at the strain free state are shown. The cell parameters averaged over the 7 independent results are $\langle a \rangle = 12.846 \pm 0.001 \text{ \AA}$, $\langle b \rangle$ (fiber axis) $= 4.887 \pm 0.001 \text{ \AA}$, $\langle c \rangle = 17.332 \pm 0.004 \text{ \AA}$, and $\langle \beta \rangle = 108.30 \pm 0.01^\circ$. The space group is $P2_1 - C_{2h}$. The averaged reliability factor $\langle R \rangle = 5.0\%$. As seen in Figure 9, the molecular chain takes essentially the fully extended all-trans conformation and the carbazoyl side-chain groups are packed well in a herringbone structure.

The crystal was stretched at a constant strain, during which a set of Weissenberg photographs were taken at room temperature. This process was repeated 6-7 times at almost the same strain value in order to check the reproducibility of the analyzed results. The change in the lattice parameters evaluated from these data are listed below and also plotted against the applied strain as shown in

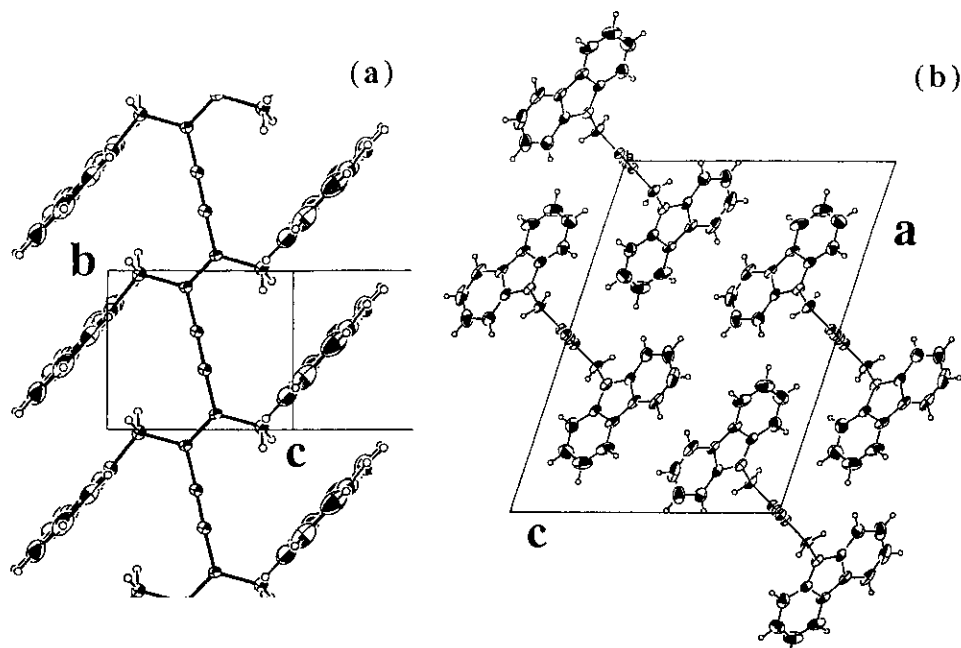


Figure 9. (a) Molecular and (b) crystal structures of PDCHD in the strain free state.¹⁴

strain/%	$a/\text{\AA}$	$b/\text{\AA}$	$c/\text{\AA}$	$\beta/^\circ$
0.0	12.846	4.887	17.332	108.30
0.25	12.826	4.899	17.317	108.30
0.39	12.824	4.906	17.318	108.30
0.67	12.788	4.919	17.286	108.33

Figure 10, where the changes are represented by percentages with the parameters obtained at the free strain as initial values (the strain along the chain axis is calculated as $(b-b_0)/b_0$, where b -axial value averaged for all the data obtained at free strain states was used as b_0). As the fiber axis b is increased by tension, the a and c axes are contracted but the angle β does not change much. These strain-induced changes in the cell constants are almost perfectly reversible. From these data we may estimate the so-called Poisson's ratios as follows:

$$v_{cb} = -(\Delta c'/c'_0)/(\Delta b/b_0) = -(\Delta c \sin \beta/c_0 \sin \beta)/(\Delta b/b_0) = 0.67$$

$$v_{ab} = -(\Delta a/a_0)/(\Delta b/b_0) = 0.38$$

where the c' is the component of the c axis perpendicular to the a axis and the angle β is practically constant. Such an exact evaluation of the

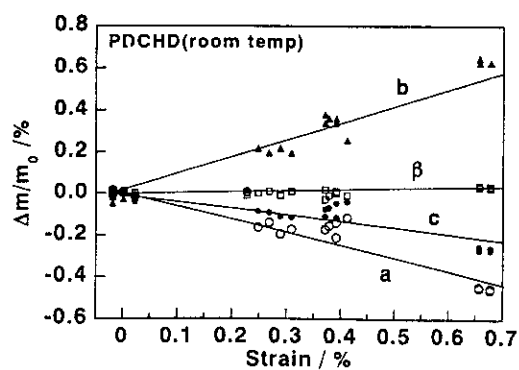


Figure 10. Stress-induced changes of lattice parameters plotted against the strain (room temperature).¹⁴

Poisson's ratio of polymer crystal is considered to be the first case as far as the authors know.

Chain Deformation and Geometrical Changes.

All the X-ray diffraction data thus collected were utilized in the refined structure analyses. The changes in the structural parameters of the molecular chains are plotted against the strain in Figures 11 and 12. As shown in Figure 11, the bond lengths of the skeletal chains R_1 (C-C) and R_2 (C≡C) are stretched almost linearly with an increase of tensile

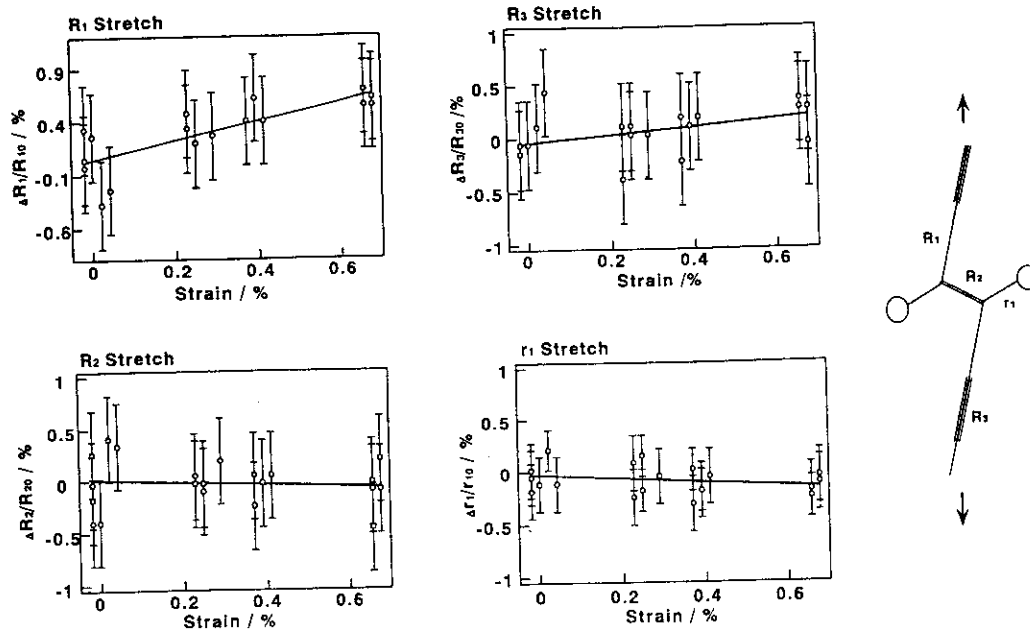


Figure 11. Strain dependence of bond lengths of PDCHD chain (room temperature).¹⁴ The definition of the bond lengths is made in the right side of this figure.

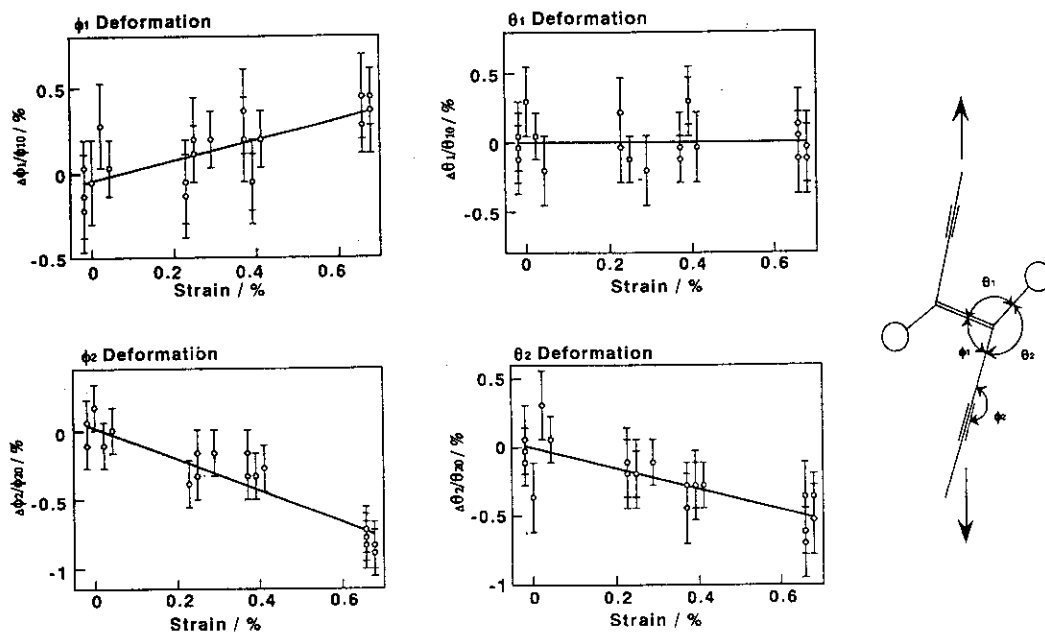


Figure 12. Strain dependence of bond angles of PDCHD chain (room temperature).¹⁴ The definition of the bond angles is made in the right side of this figure.

strain, while the bond length R_2 (C=C) and the r_1 (the bond length between the skeletal chain atom and the side group atom CH_2) are decreased to some extent. The bond length r_2 in the side group does

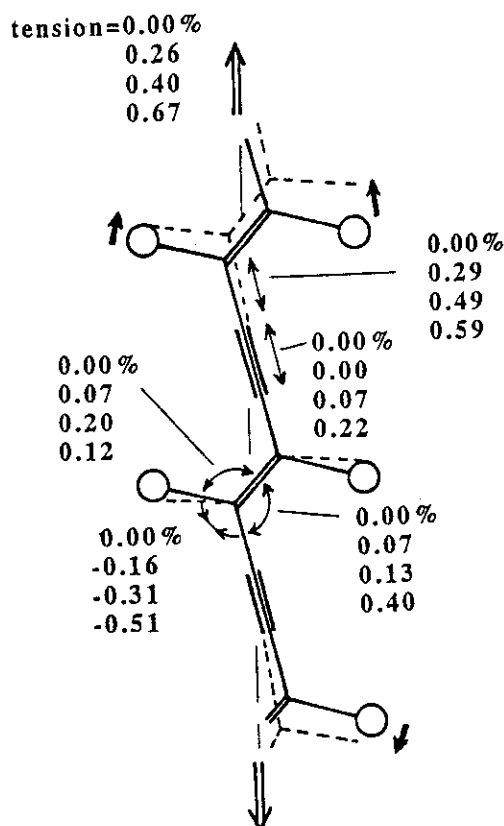


Figure 13. X-ray analyzed changes of the internal coordinates of PDCHD skeletal chain.¹⁴ Four rows of strain percentages shown at each internal coordinate correspond to the four stages of tension (from 0.0 to 0.67%).

not change at all. In Figure 12, the bond angle ϕ_1 ($\angle C-C=C$) of the skeletal zigzag chain increases but the angle θ_2 (between the bonds R_1 and r_1) decreases so as to compensate the increment of these angles ϕ_1 and θ_1 . The increase of the bond lengths and bond angles of the planar-zigzag skeletal chain subjected to the tensile stretching field can be easily imagined. The skeletal angle ϕ_2 is the angle $\angle C-C\equiv C$ of an almost linear part of the skeletal zigzag chain (178.9° at the free strain state). This angle is decreased when the chain is stretched, meaning that the long virtual bond of $C-C\equiv C-C$ is bent and wound slightly under tension. The inner structure of the side groups shows almost no geometrical change during the tensile deformation, although the orientation of the carbazolyl groups is changed slightly, as a result of the skeletal chain deformation and also due to the

compression from the surrounding chains.

Comparison of the X-ray Analyzed Deformation Mechanism with the Lattice-Dynamical Prediction. As shown in Figure 4, we predicted the atomic displacements occurring in the strained PDCHD chain on the basis of the lattice dynamical theory. The strain energy distributes preferentially to the change of the skeletal chain conformation: in particular, the distribution to the stretching of the skeletal C-C, C=C and C \equiv C bonds and the opening of the angle $\angle C=C-C$ is significant. This type of chain deformation is qualitatively in good coincidence with the above-mentioned conformational change [see Figure 13 where the changes of the parameters are listed correspondingly to the increase of the tension from 0.0 to 0.67%], although the quantitative comparison is still difficult at present because the force field employed in the theoretical calculation was too simplified¹³. However, we may say that the X-ray structural analysis has been for the first time able to confirm experimentally the molecular deformation mechanism of the PDCHD applied strain as shown in chain which was predicted theoretically on the basis of the lattice dynamical calculation.

Acknowledgment. The author would like to express his gratitude to Drs. Hiroyuki Tadokoro and Masamichi Kobayashi, professors emeritus of Osaka University, for their heartfelt encouragement. He also wishes to thank all my colleagues in performing the researches.

References

- (1) K. Tashiro, *Prog. Polym. Sci.*, **18**, 377 (1993).
- (2) K. Tashiro and M. Kobayashi, *Polymer*, **37**, 1775 (1996).
- (3) I. Sakurada and K. Kaji, *J. Polym. Sci., C*, **31**, 57 (1970).
- (4) I. Sakurada and K. Kaji, *Makromol. Chem. Suppl.*, **1**, 599 (1975).
- (5) K. Nakamae, T. Nishino, and H. Ohkubo, *J. Macromol. Sci.-Phys.*, **B30**, 1 (1991).
- (6) J. Crements, R. Jakeways, and I. M. Ward, *Polymer*, **19**, 683 (1978).
- (7) B. Brew, J. Clements, G. R. Davis, R. Jakeways, and I. M. Ward, *J. Polym. Sci., Polym. Phys. Ed.*, **17**, 351 (1979).
- (8) S. Jungnitz, R. Jakeways, and I. M. Ward, *Polymer*, **29**, 1768 (1988).
- (9) S. Jungnitz, R. Jakeways, and I. M. Ward, *Polymer*, **27**,

- 1651 (1986).
- (10) K. Nakamae and T. Nishino, *Adv. X-ray Analysis*, **35**, 545 (1992).
- (11) K. Tashiro, G. Wu, and M. Kobayashi, *Polymer*, **29**, 1768 (1988).
- (12) V. Enkelmann, *Adv. Polym. Sci.*, **63**, 91 (1984).
- (13) G. Wu, K. Tashiro, and M. Kobayashi, *Macromolecules*, **22**, 188 (1989).
- (14) K. Tashiro, H. Nishimura, and M. Kobayashi, *Macromolecules*, in press.
- (15) Z. Otwinowski, *Proceedings of the CCP4 Study Weekend: Data Collection and Processing*, 29-30 January 1993. Compiled by: Sawyer, L.; Isaacs, N.; Bailey, S. SERC Daresbury Laboratory, England, pp. 56.
- (16) W. Minor, *XDISPLAYF Program*, Purdue University, 1993.
- (17) P. Main, L. Lessinger, M. M. Woolfsom, G. Germain, J. P. Declercq, Multan 78 *A System of Computer Program for the Automatic Solution of Crystal Structures from X-ray Diffraction Data*, University of York, England and Louvain, Belgium, 1976.
- (18) R. P. Wool, R. S. Bretzlaff, B. Y. Li, C. H. Wang, and R. H. Boyd, *J. Polym. Sci., Polym. Phys. Ed.*, **24**, 1039 (1986).
- (19) G. Wu, K. Tashiro, M. Kobayashi, T. Komatsu, and K. Nakagawa, *Macromolecules*, **22**, 758 (1989).
- (20) R. J. Day, I. M. Robinson, M. Zakikhani, and R. J. Young, *Polymer*, **28**, 1833 (1987).
- (21) V. K. Mitra, W. Risen, and R. H. Baughman, *J. Chem. Phys.*, **66**, 2731 (1977).
- (22) D. N. Batchelder and D. Bloor, *J. Polym. Sci., Polym. Phys. Ed.*, **17**, 569 (1979).
- (23) R. S. Bretzlaff and R. P. Wool, *Macromolecules*, **16**, 1907 (1983).
- (24) A. I. Gubanov, *Mech. Polim.*, **5**, 771 (1967).
- (25) K. Tashiro, G. Wu, and M. Kobayashi, *J. Polym. Sci.: Part B: Polym. Phys.*, **28**, 2527 (1990).
- (26) K. Tashiro, S. Minami, G. Wu, and M. Kobayashi, *J. Polym. Sci.: Part B: Polymer Phys.*, **30**, 1143 (1992).